Atomic-Beam Scattering Studies on the Li–Hg System: Quantum Effects and Velocity Dependence of the Cross Sections*

PETER J. GROBLICKI† AND RICHARD B. BERNSTEIN

Departments of Chemistry, University of Michigan, Ann Arbor, Michigan and University of Wisconsin, Madison, Wisconsin

(Received 18 November 1964)

Measurements of the velocity dependence of the angular intensity distribution of ^{6}Li and ^{7}Li beams scattered by a crossed Hg beam are reported. The Li beams were velocity selected, the Hg beam Maxwellian. Angular intensity distributions were measured at various relative velocities (v_r) from 700–1200 m/sec, relative total cross sections (q) from $v_r = 300$ to 1350 m/sec. The differential cross sections show expected quantum interferences. Scattering patterns for ^{6}Li- and ^{7}Li–Hg are found to be identical at the same de Broglie wavelength. The over-all angular dependence of the scattering at low angles follows the $\theta^{-7/3}$ relationship characteristic of an r^{-6} long-range potential. Extrema in the total cross sections $q(v_r)$ were also observed. The experimental data were analyzed in terms of a Lennard-Jones (12, 6) potential, but it was not possible to determine a unique set of potential parameters. Comparison of observed and calculated results has yielded three nearly equivalent sets of σ, ϵ lying within the ranges $2.5 \leq \sigma \leq 3.5$ Å, $480° \leq \epsilon/k \leq 1000°$K.

I. INTRODUCTION

THE present study of the elastic scattering of lithium by mercury represents an extension and elaboration of the preliminary work of Hostettler and Bernstein[1] (HB), in which quantum effects in atom–atom scattering were first observed.

Relative differential and total cross sections for the scattering of velocity-selected atomic beams of ^{6}Li (and ^{7}Li) by a crossed thermal beam of Hg have been measured over a range of collision energies. The experimental data on the velocity dependence of the quantum effects (i.e., the interferences in the angular distributions and the extrema in the total cross sections) are compared with predictions based on a L-J (12, 6) potential. Methods are presented to correlate and interpret angular scattering patterns and high-order extrema in atom–atom impact spectra in terms of the interaction potential.

II. EXPERIMENTAL

a. Apparatus

The apparatus was essentially the same as that employed in a previous study.[2] The Li beam (the primary beam) passes through a velocity selector[3]; it is modulated at 25 cps and intersects the Hg beam at a right angle. The Li source, velocity selector, modulator, collimator, and Hg beam source and collimator are mounted on a turntable which rotates about the intersection of the Li and Hg beams. This allows the stationary detector to be set at any angle (in the plane of the two beams) with respect to the primary beam.

The Li beam is detected by conversion to ions by surface ionization on a hot, oxygenated Pt–W filament; the ions are accelerated to an electron multiplier. The output of the multiplier is fed to a cathode follower followed by a 25-cps narrow-band amplifier and phase-sensitive detector.

Small changes in the experimental arrangement used in the earlier work[1,2] were as follows.

The alkali oven slit was widened, while the Hg oven slit and collimator were narrowed; the Hg oven slit was packed with Zacharias foil. The liquid-nitrogen-cooled shield around the Hg oven was improved, reducing the amount of scattering from background Hg. A controller maintained the Hg oven temperature within ± 0.2°C, yielding a beam stability of better than 1% for several hours.

Table I lists the important apparatus dimensions. The half-widths of the source, collimator, detector, detector beam stop, umbra, half-intensity points (equivalent rectangular image), and penumbra are denoted, respectively, by: s, c, d, b, u, h, p; l_{ij} is the distance from Point i to Point j; "t" designates the scattering center or target. Primed quantities refer to half-heights.

The geometrical resolution angle is 6.8 min; the Kusch[4] resolution angle (at which the efficiency of detection of scattering is 50%) is 15 min.

b. Materials

Mallinckrodt reagent-grade mercury (>99.99%) was used.

Oak Ridge National Laboratories, suppliers of the ^{7}Li and ^{6}Li used, furnished the following analysis: isotopic

* This work received financial support from the U.S. Atomic Energy Commission, Division of Research, through Contracts AT(11-1)-321 and AT(11-1)-1328. For a fuller account, see Atomic Energy Commission Report TID-20002, November 1963, or the Ph.D. thesis of P.J.G., University of Michigan, 1964 (available from University Microfilms, Ann Arbor, Michigan).

† NSF Cooperative Fellow and Minnesota Mining and Manufacturing Company Predoctoral Fellow at the University of Michigan. Present address: Research Laboratory, General Electric Company, Schenectady, New York.

[1] H. U. Hostettler and R. B. Bernstein, Phys. Rev. Letters **5**, 318 (1960).

[2] F. A. Morse and R. B. Bernstein, J. Chem. Phys. **37**, 2019 (1962).

[3] H. U. Hostettler and R. B. Bernstein, Rev. Sci. Instr. **31**, 872 (1960).

[4] P. Kusch, J. Chem. Phys. **40**, 1 (1964).

TABLE I. Apparatus dimensions (all entries in centimeters).

	Li beam		Hg beam		Li beam		Hg beam
s	0.0266		0.080	s'	0.300		0.318
c	0.0191		0.080	c'	0.300		0.318
d	0.0254			d'	0.300		
b	0.0315			b'	0.300		
	Target	Detector	Target		Target	Detector	Target
u	0.0163	0.0010	0.0800	u'	0.300	0.300	0.318
h	0.0262	0.0713	0.1002	h'	0.411	1.10	0.398
p	0.0360	0.1416	0.1203	p'	0.522	1.91	0.478
l_{bd}	1.23						
l_{sc}	10.95		1.27	ΔV (Scattering volume) $=0.0084$ cm^3			
l_{cd}	29.35						
l_{ct}	4.05		0.32	A_d (Detector area) $=0.030$ cm^2			
l_{td}	25.3						

purity: ^{7}Li 99.994%, ^{6}Li 0.01%; other elements <0.05% each, except Sr <0.2%. Isotopic purity: ^{6}Li 96.1%, ^{7}Li 3.9%; other elements <0.05% each, except Ca and Zn <0.25%.

c. Procedure

During a typical experiment, the vacuum was 10^{-6} Torr, the temperature of the Li-beam oven was 1100°K; the Hg-beam oven was at 440°K, yielding an attenuation I_0/I in the range 1.1 to 1.7. The detection sensitivity for Li was about 10^4 atom/sec, compared with 10^2 atom/sec for K or Cs in the same apparatus. The lower sensitivity was due to the increased noise level from "bursts" of alkali ions from the high-temperature oxygenated filament.[5]

For total cross-section measurements, a Li velocity (v_1) was chosen; the primary-beam intensity was measured with the Hg beam on (I) and with the Hg beam interrupted by a shutter (I_0); this was repeated at various Li velocities.[6] For angular distributions, the zero-degree transmission (I/I_0) was measured; then the detector was placed at various angular positions with respect to the primary beam and the scattered intensity recorded, and then the 0° transmission remeasured. This procedure was repeated for each velocity and isotope. Most experiments were repeated on several days.

d. Data Processing and Method of Presentation

1. Differential Cross Sections

Experimental results were converted from measured angles θ_a and fluxes F_a, in the apparatus coordinate system (subscript a), to angles θ and fluxes F, in the center-of-mass (c.m.), system, using standard equations[2,7] assuming monoenergetic beams.[8]

The problem of obtaining absolute values of the differential cross section has not yet been solved; therefore, in practice, the quantity $D(\theta)$ [proportioned to $d\sigma(\theta)/d\Omega$] is derived from the experimental measurements.[2]

Both theoretical and experimental angular distributions show decreases in intensity of many orders of magnitude as the scattering angle is increased. Even on a semilog plot of intensity vs angle, small quantum effects (undulations) are difficult to observe in the presence of a rapidly changing monotonic (classical) background. For a potential with a long range r^{-6} dependence, the classical low-angle scattering is given[7] by the Kennard[9] formula

$$d\sigma(\theta)/d\Omega \propto \theta^{-\frac{4}{3}} \csc\theta \cong \theta^{-\frac{7}{3}}. \quad (1)$$

Angular distributions for the K– and Cs–Hg systems had been found[2] to accord with this relation for $\theta \lesssim 10°$, suggesting the utility of a function

$$G(\theta) \equiv \theta^{\frac{4}{3}} \sin\theta D(\theta) \cong \theta^{\frac{7}{3}} D(\theta), \quad (2)$$

which should be essentially constant at low angles, except where deviations from a smooth $\theta^{-\frac{7}{3}}$ dependence occur. This allows detection of quantum undulations with great sensitivity. This method of presentation has therefore been adopted.

2. Total Cross Sections

Previous work[10] has shown that total cross-section (Q) data may best be compared with theory when

[5] R. E. Minturn, S. Datz, and E. H. Taylor, J. Appl. Phys. **31**, 876 (1960).

[6] Measurements were considered valid only if those taken near the end of the series reproduced those taken at the beginning.

[7] R. B. Bernstein, Science **144**, 141 (1964).

[8] The Li beam has a velocity spread at half-intensity of 4.7% of the nominal velocity, and the Hg beam is Maxwellian. Due to the heavy mass and consequently low average speed of the Hg, this introduces only a moderate spread in the relative velocity v_r.

[9] E. H. Kennard, *Kinetic Theory of Gases* (McGraw-Hill Book Company, Inc., New York, 1938).

[10] R. B. Bernstein, J. Chem. Phys. **38**, 2599 (1963).

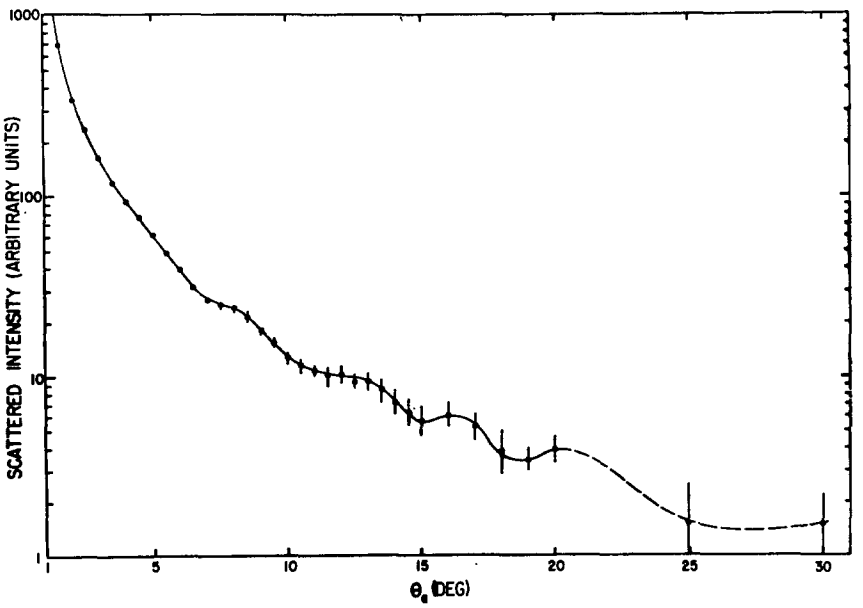

FIG. 1. Typical experimental data for the scattering of ^{6}Li by Hg for $v_r = 1213$ m/sec.

presented as plots of $v_r^{\frac{1}{3}}Q(v_r)$ vs $1/v_r$. Consistent with HB, the problem of evaluating the number density (n_2) path length (l) product for the secondary beam is circumvented by defining an experimentally measureable *relative* total cross section $q(\bar{v}_r)$:

$$q(\bar{v}_r) = (v_1/\bar{v}_r)\,\log(I_0/I) \propto Q(v_1)/n_2 l, \qquad (3)$$

where $\bar{v}_r$ is an average relative velocity approximated by

$$\bar{v}_r = (v_1^2 + \bar{v}_2^2)^{\frac{1}{2}}, \qquad (4)$$

with $\bar{v}_2$, the average speed of the secondary beam molecules taken as

$$\bar{v}_2 = 1.33(2kT_2/m_2)^{\frac{1}{2}}. \qquad (5)$$

The present experimental results are shown as log-log plots of $\bar{v}_r^{\frac{1}{3}}q(\bar{v}_r)$ vs $1/\bar{v}_r$. The logarithmic scale allows the ordinate to be considered as the desirable $\log v_r^{\frac{1}{3}}Q$ plus some constant related to the unknown $n_2 l$ product.

Note added in proof: Recent work [A. R. Blythe, A. E. Grosser, and R. B. Bernstein, J. Chem. Phys. **41**, 1917 (1964)] has shown that in place of $\bar{v}_2^2$ in Eq. (4) it is more correct to use α_2^2 $(=2kT_2/m_2)$.

III. EXPERIMENTAL RESULTS

1. *Differential Cross Sections*

A semilogarithmic plot of the original data for a typical experiment is shown in Fig. 1. The vertical lines show the uncertainty (due to signal to noise) of each point. On this type of plot, undulations appear as "shoulders" on the decreasing background curve. Since the curve shapes are identical for the curve drawn through the points representing the most probable value of the intensity and a curve drawn through the ends of the ranges, only the most probable value is used in subsequent calculations. Figure 2 is a log-log plot of the same data after conversion to the c.m. system. Due to the small mass ratio (Li/Hg), the scattering angles are nearly the same in the c.m. and apparatus systems; in this example, θ_a of 30.0° corresponds to θ of 32.5°. The low-angle scattering falls close to the line drawn with the theoretical classical slope of $-\frac{7}{3}$, suggesting that the $G(\theta)$ curve might be nearly horizontal. Figure 3 shows the plot of $G(\theta)$, with the undulations now appearing as sinusoidallike deviations from a smooth curve. Using this presenta-

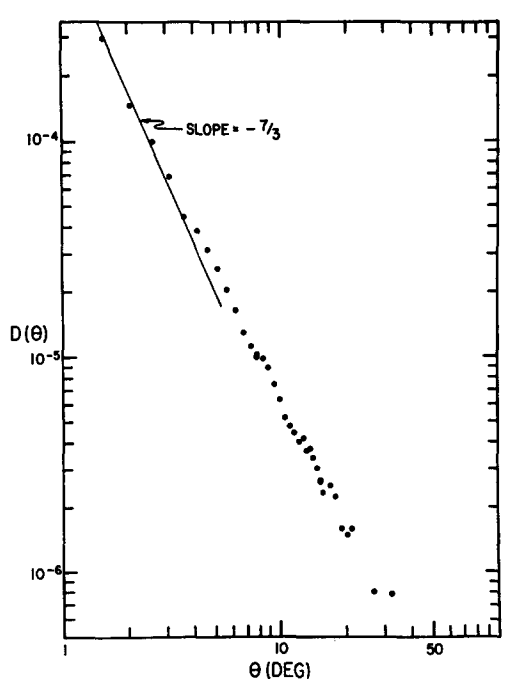

FIG. 2. Typical data: log-log plot of the data of Fig. 1, after conversion to the center-of-mass system.

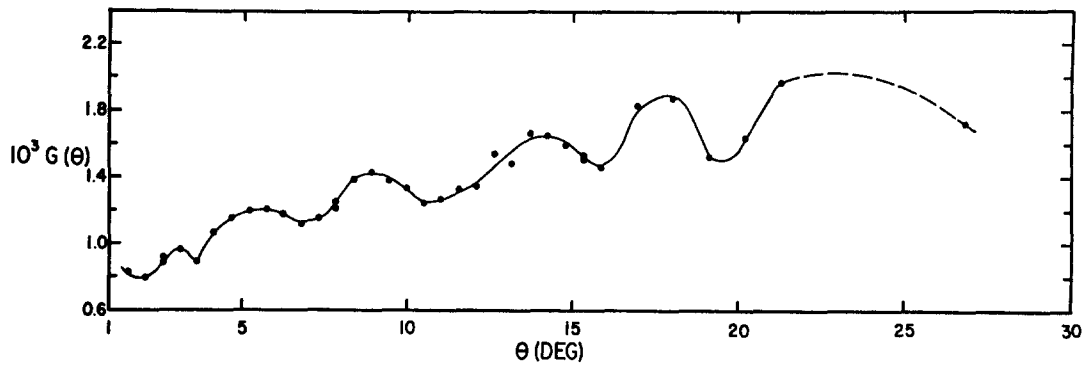

FIG. 3. Typical data: $G(\theta)$ presentation of the same data (Fig. 2) showing resolution of extrema.

tion, the angular positions of the undulations can be located to within about $\pm 0.5°$.

Angular distributions were measured for ^{6}Li and ^{7}Li at several relative velocities. The results are shown in Figs. 4 and 5. Due to difficulties in duplicating the Hg-beam intensity, it is not possible to superimpose plots of replicate experiments (i.e., carried out at the same v_r) to obtain a unique "scattering pattern." If, however, the experiments at the same v_r are plotted separately on the same angular scale, as in Figs. 4 and 5, one can readily estimate the most probable extrema positions. This has been done, with uncertainties indicated by the length of the horizontal bars at the bottom of the figures. The numbers (1, 2, ···, 10) near the points at the bottom of each graph give the "best experimental weights" of the various points, with high numbers implying a large number of replicate experiments (or exceptionally good agreement between a smaller number).

Table II and Fig. 6 summarize the data. The entries in Table II record the most probable positions of each maximum or minimum; an estimate of the uncertainty in position may be obtained by inspection of Figs. 4 and 5. In Fig. 6, the pattern of maxima and minima at each value of v_r is plotted at the corresponding value of $\log k (k \equiv \mu v_r/\hbar$, where μ is the reduced mass). It is of interest to note the similarity in the scattering patterns for ^{6}Li and ^{7}Li when results are compared at the same k (*not* the case at the same v_r).

The earlier measurements of HB (using natural isotopic Li) agree well with the ^{7}Li data of the present more extensive and more precise experiments.

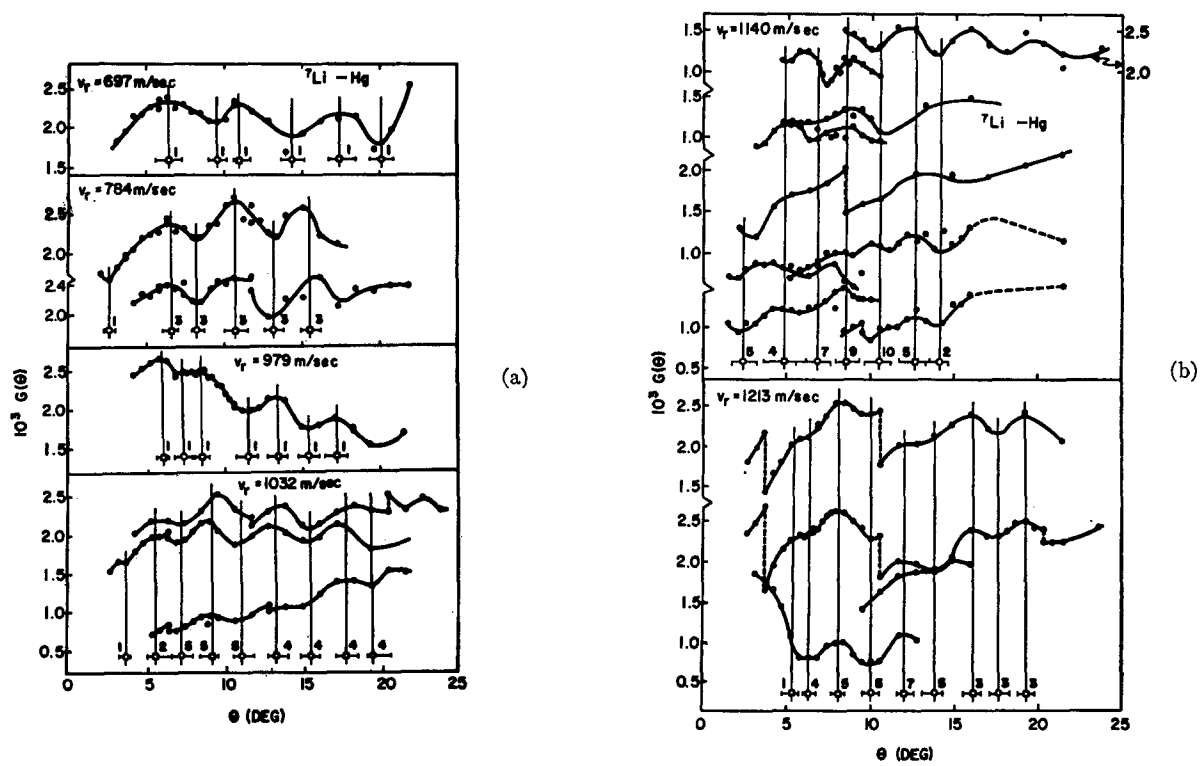

FIG. 4. Experimental data for the scattering of ^{7}Li by Hg at various relative velocities. Vertical discontinuities are not significant. See text *re* assignment of extrema angles.

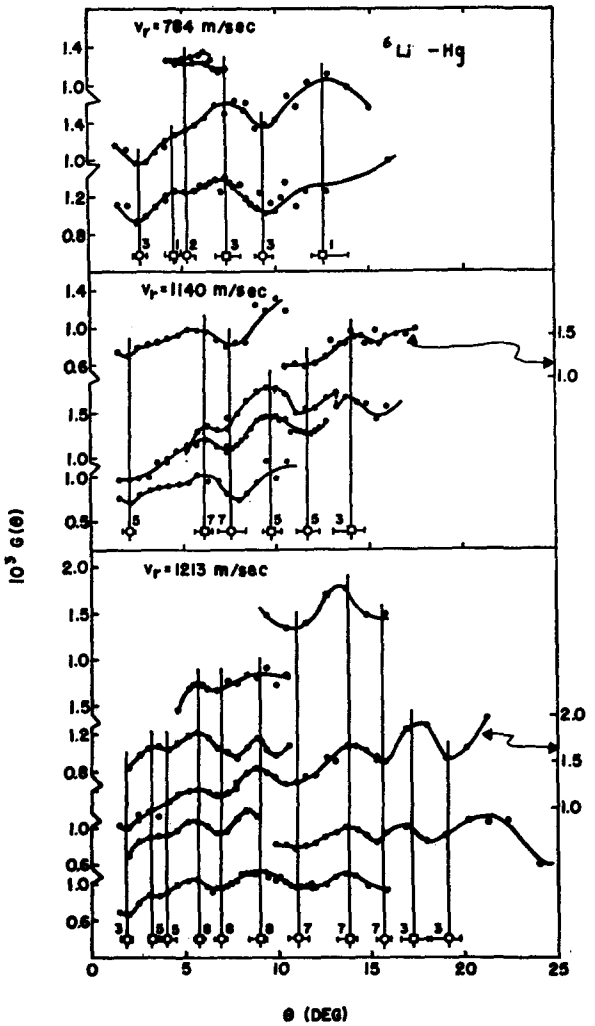

FIG. 5. Experimental data for the scattering of ^{6}Li by Hg at various relative velocities, as in Fig. 4.

2. *Total Cross Sections*

Relative total cross-section measurements were made for both isotopes of Li. Figure 7 shows a set of typical original data, I/I_0 versus v_{Li}. This type of plot shows

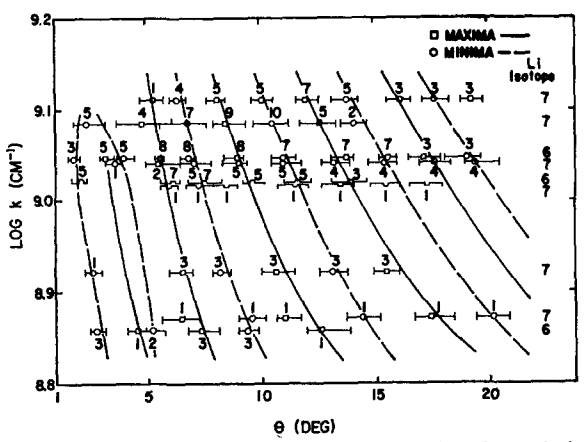

FIG. 6. Summary of experimental data, showing the variation of scattering patterns with wavenumber k.

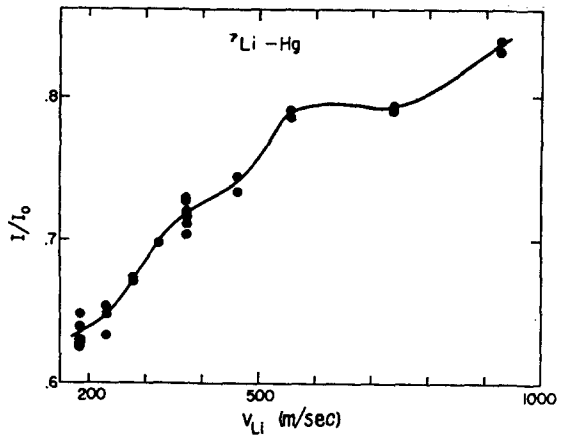

FIG. 7. Typical raw data for total cross sections. Attenuation of ^{7}Li by Hg.

some hint of extrema, which are made apparent by Figs. 8 and 9, which show the data for ^{6}Li and ^{7}Li, respectively. The lower sections of these graphs also show various predicted patterns of extrema in the total cross sections (to be discussed later). Unfortunately the imprecision in the data is such as to preclude the determination of extrema velocities with any degree of reliability.

IV. THEORETICAL DISCUSSION

The goal of a scattering study such as the present one is to evaluate the interaction potential from the

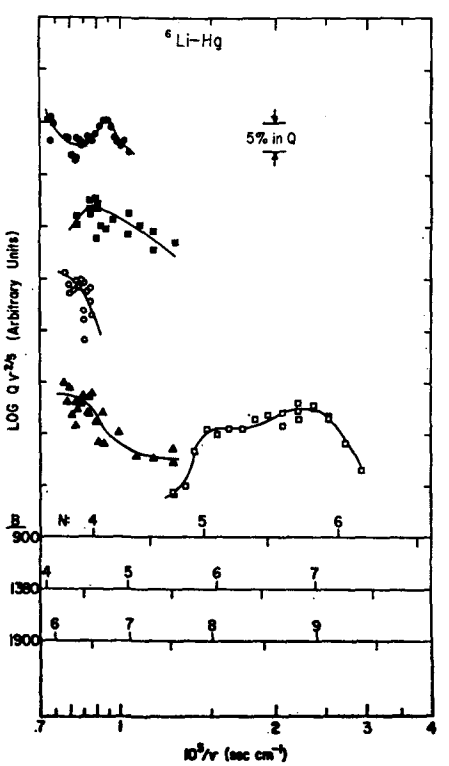

FIG. 8. Total cross-section data for ^{6}Li–Hg. Each set of points represents a separate run. The lower portion shows theoretical predictions of the positions of the extrema (see text).

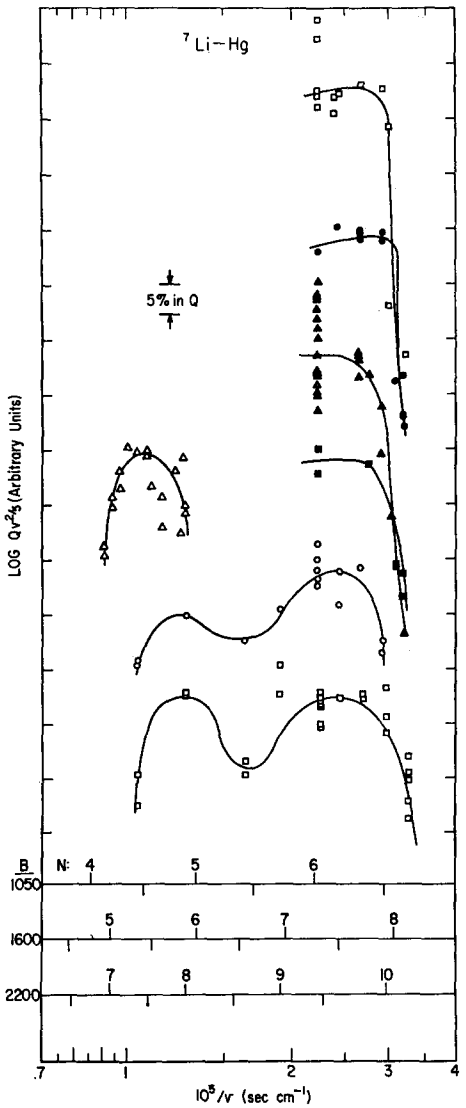

FIG. 9. Total cross-section data for ^{7}Li–Hg, as in Fig. 8.

scattering cross sections. In previous studies of heavy-particle systems at thermal energies, quantum effects in $d\sigma(\theta)/d\Omega$ have been unresolved, only the gross, essentially classical features being observed.[2,11,12a] Thus, it has been possible to fit the "shape" of the observed angular distributions[13,14] with the use of simple two- or three-parameter potential functions and classical mechanics alone. These methods are, however, fairly insensitive, and considerable ambiguity in the potential remains even after a "successful" fit to an angular distribution of presently attainable accuracy. (This is basically due to the fact that the smooth, low-resolution "shape" contains relatively few information bits.) Also, of course, the derived parameters themselves depend strongly upon the assumed functional form of $V(r)$.

For low-energy scattering of low reduced-mass systems (for which quantum effects should be important) a fair number of quantum calculations have now been carried out,[1,15–17] using two- to five-parameter potentials. Unfortunately, with the exception of the data of Ref. 1, the only relevant observations are the essentially unresolved angular distributions of Knauer[18] for He– and H_2–Hg and Zabel[19] for He– and H_2–He. It is obvious that when quantum effects can indeed be resolved, the angular scattering patterns offer a rich source of information. For example, in the present instance considering only the *angular positions* of the extrema in the $G(\theta)$ patterns [i.e., for the moment ignoring the over-all

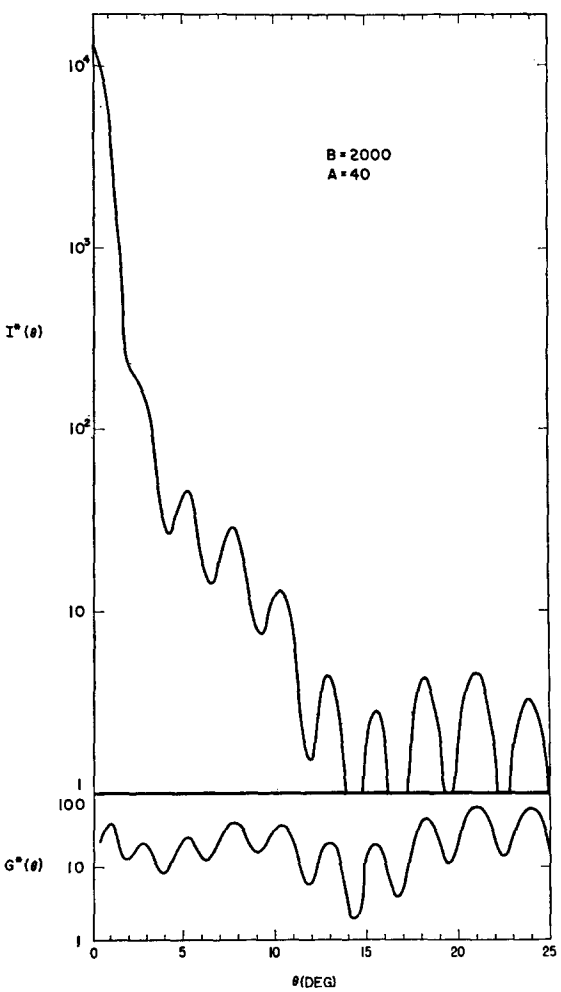

FIG. 10. Comparison of $I^*(\theta)$ and $G^*(\theta)$ presentations of typical calculated angular distributions.

[11] D. Beck, J. Chem. Phys. **37**, 2884 (1962).
[12] (a) E. Gersing, E. Hundhausen, and H. Pauly, Z. Physik. **171**, 349 (1963); see also (b) E. Hundhausen and H. Pauly, Z. Naturforsch **19a**, 810 (1964).
[13] E. A. Mason, J. Chem. Phys. **26**, 667 (1957).
[14] H. U. Hostettler and R. B. Bernstein, J. Chem. Phys. **31**, 1422 (1959).
[15] R. B. Bernstein, J. Chem. Phys. **33**, 795 (1960); **34**, 361 (1961).
[16] (a) C. R. Mueller and R. P. Marchi, J. Chem. Phys. **38**, 745 (1963); (b) W. A. Sanders and C. R. Mueller, *ibid.* **39**, 2572 (1963).
[17] R. B. Bernstein and F. A. Morse, J. Chem. Phys. **40**, 917 (1964).
[18] F. Knauer, Z. Physik **80**, 80 (1933); **90**, 559 (1934).
[19] R. M. Zabel, Phys. Rev. **44**, 53 (1953).

TABLE II. Angular positions of extrema in experimental $G(\theta)$ curves.

	^{6}Li			^{7}Li					
v_r (m/sec)	784	1140	1213	697	784	979	1032	1140	1213
$\log_{10}k$ (cm^{-1})	8.858	9.021	9.048	8.872	8.932	9.019	9.042	9.086	9.112
Min	2.8[a]	2.1	1.8		2.6			2.4	
Max	4.6		3.2						
Min	5.3		4.0				3.6		
Max	7.4	6.1	5.7	6.5	6.6	6.0	5.5	4.8	5.3
Min	9.4	7.5	6.9	9.6	8.2	7.3	7.1	6.8	6.3
Max	12.6	9.7	9.0	11.0	10.7	8.5	9.1	8.5	8.1
Min		11.6	11.0	14.4	13.2	11.5	11.0	10.5	10.0
Max		14.0	13.8	17.5	15.5	13.4	13.2	12.6	12.0
Min			15.6	20.2		15.4	15.4	14.1	13.8
Max			17.2			17.2	17.7		16.1
Min			19.1				19.4		17.6
Max									19.3

[a] Estimates of the uncertainty in these positions are given on Figs. 4 and 5.

shape of $d\sigma(\theta)/d\Omega$ and the total cross-section data], 67 information bits (Table II) are available with which to attempt the "inversion"[20] operation (cross sections→ potential).

This "overdetermination" of a few-parameter potential has, however, not been fully exploited in the present study, because of the rather primitive inversion technique currently practical. The present procedure (which may be termed synthetic rather than analytic) may be summarized as follows:

(1) Several "reasonable" values of the quantum parameter[15] $B \equiv 2\mu\epsilon\sigma^2/\hbar^2$ were chosen.

(2) A complete set of phase shifts $\eta_l(A)$ were calculated at various values of the velocity parameter[15] $A \equiv k\sigma$ for each value of B, using the exact (RKG integration) method to compute a fraction (approximately $\frac{1}{4}$) of the phases, the reduced-phase (Q-i-K curves[15]) method plus interpolation for the remainder of the low-order phases, and the J–B approximation for the higher-order phases.

(3) Reduced angular distributions $I^*(\theta) \equiv I(\theta)/\pi\sigma^2$ as well as $G^*(\theta) \equiv I^*(\theta)\theta^{\frac{1}{2}} \sin\theta$ were computed for each case using the standard equations.

(4) Reduced total cross sections $Q^*(A) = Q(A)/\pi\sigma^2$ were calculated for each B.

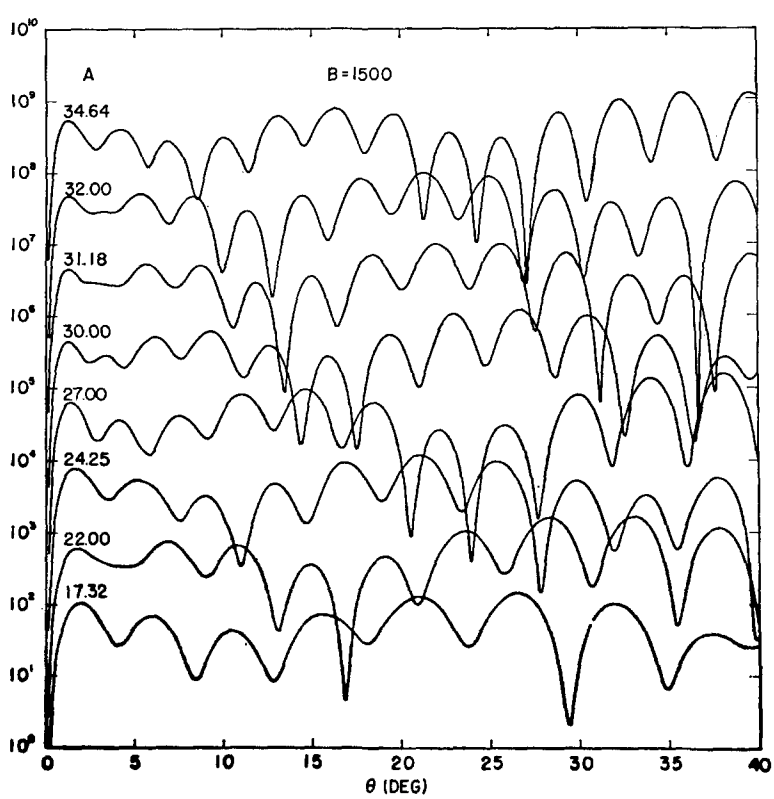

FIG. 11. Typical family of calculated $G^*(\theta)$ $G^*(_p)$ curves; $B=1500$.

[20] The formal solutions to the inversion problem have not yet been applied to a practical example in the atomic scattering field: (a) E. A. Hylleraas, Physica Mathematica University Oslo, Rept. No. 19 (1963); see also the review: (b) L. D. Faddeyev, J. Math. Phys. 4, 72 (1963).

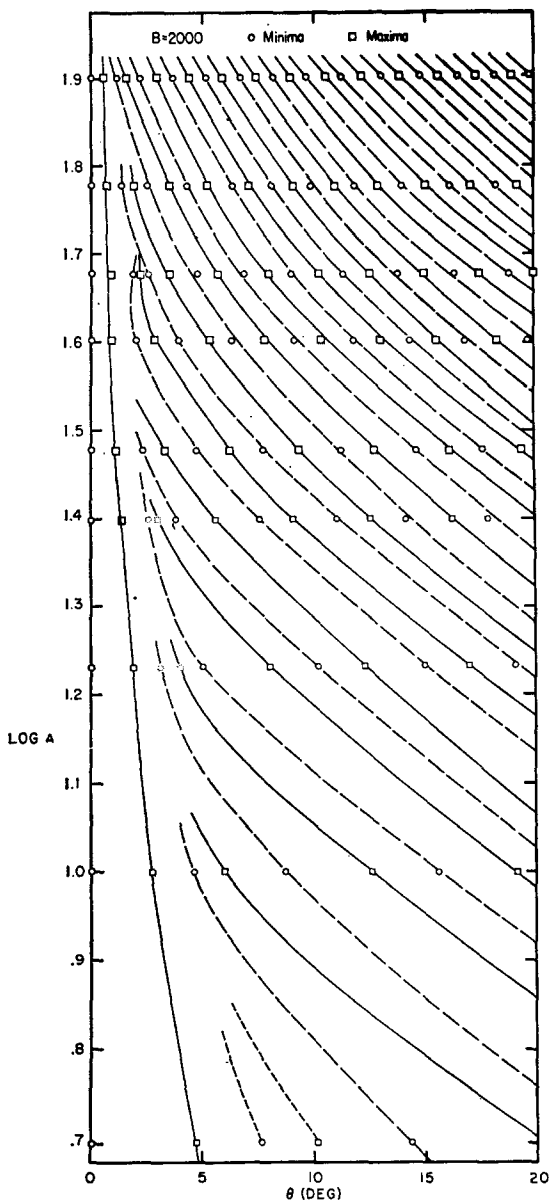

FIG. 12. Calculated scattering patterns for $B=2000$. The points are the computed values.

Figure 10 shows a typical calculated angular distribution curve, $I^*(\theta)$, for $B=2000$, $A=40$; also shown is a semilog plot of the corresponding $G^*(\theta)$ curve. A typical family of $G^*(\theta)$ curves ($\log G^*$ vs θ) is shown in Fig. 11. The ordinate scale for each successive curve is displaced vertically by one log unit.

It is interesting to note the disappearance of the second maximum as A is increased from 27($B=1500$). When a maximum–minimum pair is just barely detectable as a shoulder on the G^* curve a dotted symbol is used in subsequent graphs. Figures 12–14 display the positions of the maxima and minima as a function of angle for $B=2000$, 1500, and 1000. The vertical placement of each horizontal line of points (from the calculated scattering pattern) is determined by $\log A$. Lines are then drawn through corresponding undulations. Although relatively insensitive to B, the curve shape and spacing depends very strongly upon A. This presentation should allow the prediction of the scattering patterns for any value of A within the range for which the patterns were calculated.

If the experimental scattering patterns can be fitted to the theoretical ones, then the vertical position at which a good fit is obtained should determine σ directly. The set of experimental points[21] shown in Fig. 6 was superimposed upon each theoretical scattering pattern curve at a number of positions corresponding to values of σ ranging from 2 to 6 Å.

Figure 14 shows the superposition of the experimental data on the calculated pattern at which the *best* agreement between theory and experiment was found (i.e., for $B=1000$). The maximum possible sum of the "weights" of the experimental points is 250; unfortunately, even for the best fit, only about 160/250 of the total weight agrees with theory.

Table III lists the values of σ obtained by this superposition procedure. From the values of σ and B, it is possible to calculate a value for ϵ (using μ for ^{7}Li); these values of ϵ are also listed. As mentioned above, the fit corresponding to Set 1 is somewhat better, so that those parameters are to be considered the preferred set.

The rather poor quality of the fit with any of the calculated scattering patterns raises some doubt as to the validity of the L-J (12, 6) potential on which the analysis is based, in accord with the findings of Mueller,[16] Pauly,[22] and others.

With regard to the total cross sections (Figs 8–9), the precision of the available data does not warrant a detailed comparison of theory and experiment (such as that carried out for Li–Xe, etc.[23]). Instead, the data are tested for compatibility with the σ and ϵ deduced from the differential cross sections.

The lower sections of Figs. 8 and 9 show theoretical extrema patterns calculated using the procedure of

TABLE III. Potential parameters determined from angular distributions.

	Set 1	Set 2	Set 3
B(nominal)	1000	1500	2000
σ (Å)	2.52	3.47	2.80
$10^{14}\epsilon$(erg)	7.8	6.2	12.6

[21] No attempt was made to fit the experimental points for each isotope separately. The experimental points for both isotopes agreed well, and the theoretical curves appear to be insensitive enough to B so that the 14% difference in B due to the different reduced masses should not affect the results.

[22] R. Düren and H. Pauly, Z. Physik **175**, 227 (1963); **177**, 146 (1964).

[23] E. W. Rothe, P. K. Rol, and R. B. Bernstein, Phys. Rev. **130**, 2333 (1963).

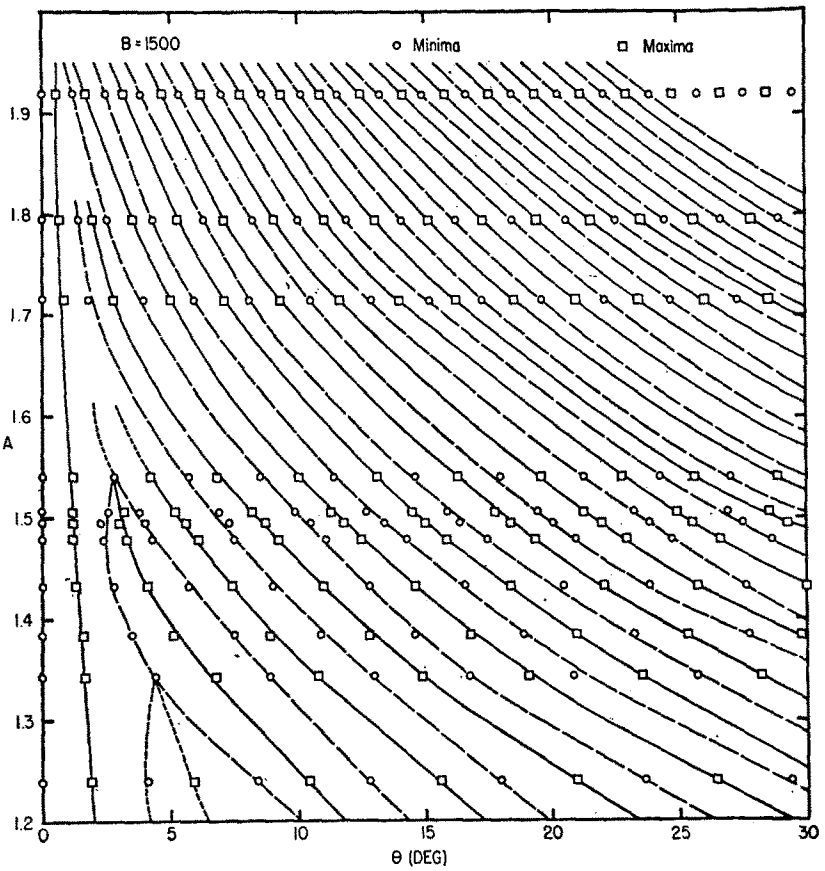

FIG. 13. Calculated scattering patterns for $B=1500$, derived from Fig. 11. The points are the computed values.

Ref. 10. Because of the curvature in the plots of N vs v^{-1} for high B systems, there is a significant isotope effect upon the extrema velocities. For each nominal value of B at which the angular distributions were fitted, theoretical extrema patterns were fitted to the experimental observations, such that the theoretical patterns fit the data *and* maintain the proper ratio of the B's. From this comparison, values of $\epsilon\sigma$ were deduced.

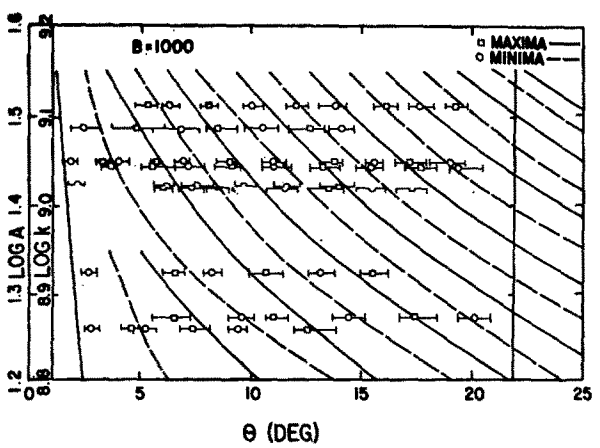

FIG. 14. Comparison of experimental and calculated scattering patterns; $B=1000$. Here the points are the *experimental* values (from Fig. 6) while the solid curves represent the computations.

Table IV gives the values of B, σ, and $\epsilon\sigma$ at which a reasonable fit was obtained between experimental and calculated extrema patterns. The $\epsilon\sigma$ product thus obtained from the total cross sections may be combined with the σ obtained from the angular distributions to obtain a "check" value of B (self-consistency):

$$B_{\text{check}}=(2\mu/\hbar^2)(\epsilon\sigma)_{\text{tot}}\sigma_{\text{ang}}. \tag{6}$$

Table V summarizes the results of the present investigation for the Li–Hg system. As mentioned earlier, Set 1 is to be preferred.[24]

TABLE IV. Parameters obtained using combined data on total cross sections and angular distributions.

Li isotope	B (assumed)	Set No.	σ (Å)	$10^{21}\times\epsilon\sigma$ (erg·cm)	B_{check}
6	900	1	2.52	1.95	855
	1380	2	3.47	2.24	1350
	1900	3	2.80	3.85	1880
7	1050	1	2.52	1.95	1010
	1600	2	3.47	2.35	1645
	2200	3	2.80	3.95	2240

[24] Unfortunately the C constant ($C=4\epsilon\sigma^6$) corresponding to Set 1 is only 80×10^{60} erg·cm^6 compared to 460×10^{60} erg·cm^6 for Set 2; a theoretical estimate (Slater–Kirkwood type; using polarizabilities $\alpha_{\text{Hg}}=5.1$, $\alpha_{\text{Li}}=22$ Å^3) is 450×10^{60} erg·cm^6.

TABLE V. Summary of L-J (12,6) parameters.

Set No.	Nominal B	σ (Å)	$10^{21}\times\epsilon\sigma$ (erg·cm)	ϵ/k (°K)
1	1000	2.52	1.95	560
2	1500	3.47	2.30	480
3	2000	2.80	3.90	1008

This is the first system for which both the extrema in the total cross sections and the undulations in the differential cross sections have been observed. In spite of the problems encountered, the methods of analyzing the data allow reasonable limits to be placed on the values of σ and ϵ: 2.5 Å$\leq\sigma\leq$3.5 Å and 480°$<\epsilon/k\leq$ 1008°K. In the Li–rare-gas systems[23] values of σ exceeding 4.5 Å and $\epsilon/k\leq$150°K were found in all cases. The present results indicate a considerably greater depth of the Li–Hg potential well and a significantly smaller equilibrium interatomic separation, implying that the LiHg ($^2\Sigma^+$) molecule is more tightly bound than the comparable Li–rare-gas diatom. (The compound LiHg is known from studies of the Li–Hg phase diagram.[25])

From experiments on rainbow scattering, the well depths for the K–Hg and Cs–Hg systems have been estimated.[2] For these systems, the ϵ/k values were 539° and 558°K, respectively. Pauly[12b] has recently reported values for Na–, K–, and Rb–Hg: 572°, 544°, and 529°K, respectively. The present ϵ/k results for Li–Hg (Sets 1 and 2) are similar. This raises the interesting possibility that the well depth for the alkali–Hg systems may be nearly constant.

V. SUMMARY AND CONCLUDING REMARKS

The velocity dependence of the angular distribution of Li scattered by Hg has been measured by the atomic-beam technique. The angular distribution showed evidence of oscillatory quantum interferences. By proper selection of the velocity for each of the isotopic Li species (i.e., choosing the same de Broglie wavelength for the system ^{6}Li–Hg and ^{7}Li–Hg), the same scattering pattern was observed for the different isotopes at constant λ. In addition, the gross angular dependence of the low angle scattering is in accord with predictions based on an assumed long-range inverse-sixth-power dependence of the attractive potential. From the comparison of theoretical predictions with the experimentally observed undulation patterns in the angular distributions (at various relative velocities), assuming a L-J (12, 6) potential, it was found that σ lies in the range 2.5 to 3.5 Å.

Values of the relative total cross section have also been measured as a function of velocity. The atom–atom impact spectra exhibit extrema, as expected on theoretical grounds. Although these measurements are of marginal precision, they allow a crude determination of the product $\epsilon\sigma$, from which the value of ϵ may be estimated. The values of ϵ/k so determined range from 480° to 1000°K.

The present study indicates that only moderate improvements in molecular-beam scattering techniques would yield sufficient precision to enable an "overdetermination" of the potential for light-atom systems. Given more precise data on the velocity dependence of the total and differential elastic scattering cross sections, it should be possible, in the future, to extract potential parameters of high accuracy which could be useful in extending our knowledge of interatomic forces.

ACKNOWLEDGMENTS

The authors appreciate the significant contributions of Dr. H. U. Hostettler, who was primarily responsible for the design and construction of the original apparatus and for the early measurements on the Li–Hg system. The advice of Dr. F. A. Morse during the early stages of this work is also appreciated. The assistance of C. Charters, A. Flank, A. Graube, A. Korreck, and F. Parker in the data processing is gratefully acknowledged, as is a grant of computer time by the University of Michigan Computing Center.

[25] *Liquid Metals Handbook*, edited by R. N. Lyon [Office of Naval Research–Atomic Energy Commission (U.S.) Government Printing Office, 1954].